Fermilab

TM-1232
0102.000

COMBINED FUNCTION MAGNET PROFILE DESIGN

S.C. Snowdon

November 1983

INTRODUCTION

Conformal mapping has been used in the past to generate magnet poleface contours.[1] The present effort extends a notion considered previously in which a plane of symmetry was introduced. One further mapping permits the plane of symmetry to be transformed into a curved surface of bifurcation. A magnetostatic problem set on one side may be continued into the other side thereby providing an exact solution on both sides. An application is made for the Beijing Synchrotron[2] booster magnet.

COMBINED FUNCTION MAGNET

The desired poleface contour is considered to be one of the surfaces for which the magnetostatic potential V is a constant. As V approaches some limit V_0 the contour is usually reduced to a sequence of straight lines in the z-plane which are then related to the real axis of the s-plane by a suitable transformation.[3] For a combined function magnet the previous z-plane is designated as the r-plane and a transformation is made to the z-plane using $r = z+\frac{1}{2}kz^2+\frac{1}{6}k'z^3$. This distorts the generator elements ($V=V_0$) from linear to curved segments. The mappings are illustrated in Figures (1-3).

Quantitatively one bends the real axis of the s-plane into a polygon whose interior angles are indicated in Figure 1. The result in the r-plane may be written as[4]

$$r = \frac{g_1}{C_1} \int \frac{\left(1+\frac{1}{\alpha}\right)\left(1+\frac{s}{\gamma}\right)}{(1+s)^{2-\frac{\omega}{\pi}}\left(1-\frac{s}{\delta}\right)^{\frac{1}{2}}\left(s^2-\tau^2\right)^{\frac{1}{2}}}\, ds\,, \tag{1}$$

where $-\alpha$, -1, $-\gamma$, $-\tau$, τ, and δ are bend points in the s-plane. For the magnetostatic problem shown in Figure 1 where U is the stream function and V is the potential function, the result of transforming to the r-plane represents a symmetrical dipole and is shown in Figure 2.

To produce the right hand side of a combined function magnet the r-plane is distorted into the z-plane using

$$r = z + \tfrac{1}{2} k z^2 + \tfrac{1}{6} k' z^3, \tag{2}$$

where k is the field index and k' is the gradient index.

Magnetostatic considerations are readily inserted into a w-plane which is obtained from the s-plane using bends only at $\pm\tau$. Thus

$$w = \int \frac{ds}{\left(s^2-\tau^2\right)^{\frac{1}{2}}} \qquad \text{or} \qquad s = \tau \cos(i w)\,. \tag{3}$$

From Figure 4 it may be seen that a uniform field in the w-plane yields an excitation in the s-plane in which the exciting currents are at infinity. The complex potential is

$$W = U + iV = \frac{V_0}{\pi} w\,. \tag{4}$$

This representation of the complex potential will be modified later in order to locate the excitation current at a finite distance.

Starting with the w-plane and defining for convenience

$$G(s) = \frac{(1+s)^{2-\frac{\omega}{\pi}}\left(1-\frac{s}{\delta}\right)^{\frac{1}{2}}}{\left(1+\frac{s}{\alpha}\right)\left(1+\frac{s}{\gamma}\right)} \tag{5}$$

one has

$$r = \frac{q_1}{C_1}\int \frac{dw}{G(s)}\,, \qquad (6)$$

and for the magnetic field

$$H^{*} = H_x - iH_y = i\frac{dW}{dz} = i\frac{V_0}{\pi}\cdot\frac{C_1}{q_1}G(s)\cdot\left[1 + kz + \tfrac{1}{2}k'z^2\right]. \qquad (7)$$

The constant q_1 as shown in Figure 2 is the imaginary part of r on the surface $V = V_1$ associated with the curve of bifurcation $U = 0$. By integrating in Eq. (6) along the line $\rho = 0$ from $\phi = 0$ to $\phi = \phi_1$ one obtains C_1. Thus

$$C_1 = \int_0^{\varphi_1}\frac{d\varphi}{G(\xi)}\,, \qquad (8)$$

where

$$\xi = \tau\cos\varphi. \qquad (9)$$

Equation (7) may be used to relate V_0 to an assigned magnetic induction B_0 at the origin $x = 0$, $y = 0$

$$H_y(0,0) = -\frac{V_0}{\pi}\,\frac{C_1}{q_1}\,G(\tau) = -B_0\,. \qquad (10)$$

To find the magnetic field gradient on the median plane differentiate Eq. (7) with respect to z, set $y = 0$ and take the imaginary part. Thus

$$\frac{H_y'(x)}{H_y(0)} = \frac{G(\xi)}{G(\tau)}\left\{k + k'x + \left(1 + kx + \tfrac{1}{2}k'x^2\right)^2\frac{C_1}{q_1}\sqrt{\xi^2 - \tau^2}\,G(\xi)\frac{d\ln G}{d\xi}\right\}, \qquad (11)$$

where from Eq. (6)

$$\rho = \frac{q_1}{C_1}\int_0^{\rho}\frac{d\rho}{G(\xi)}\,, \qquad (12)$$

with

$$\xi = \tau \cosh \rho , \tag{13}$$

and from Eq. (2)

$$p = x + \frac{1}{2} k x^2 + \frac{1}{6} k' x^3 \tag{14}$$

The contour represented by $V = V_1$ or $\phi = \phi_1$ may be found using Eq. (6) with

$$s = \tau \cos\left[i(\rho + i\phi_1)\right] . \tag{15}$$

Thus

$$r = i\phi_1 + \frac{\phi_1}{C_1} \int_0^{\rho} \frac{d\rho}{G(s)} , \tag{16}$$

where r is related to z by Eq. (2). If Eq. (7) is evaluated for values of s in Eq. (15) the magnetic field may be found along the contour. Note that ρ is a convenient variable for parametrizing all variables of interest.

Any method of numerical integration of Eqs. (8), (12), and (16) will yield results for the desired quantities provided that B_0 k k' q_1 ω ϕ_1 δ α γ and τ are given. However, the design problem is to find these constants in terms of physically specifiable characteristics of the magnet and its field. By adding two more unknowns, ρ_0 the value of ρ at the maximum excursion of the gradient from the "ideal" gradient, and ρ_e the value of ρ at the maximum extent of the "good field" region, one may utilize information to be specified at these points. Table 1 includes a comparison of these unknowns with quantities and conditions to be specified. Note that the "ideal" field on the median plane is

$$H_y = -B_o\left(1 + kx + \tfrac{1}{2}k'x^2\right),$$

and that the deviation of the actual median plane field from the "ideal" field is

$$\frac{\Delta H_y}{H_{yo}} = \left[\frac{G(\xi)}{G(\tau)} - 1\right]\cdot\left(1 + kx + \tfrac{1}{2}k'x^2\right). \qquad (17)$$

Table 1. Comparison of Unknowns with Given Quantities

Unknown	Given	Unknown	Given
B_o	B_o	α	$\Delta H_y'/H_{yo}$ at ρ_o
k	k	γ	$\Delta H_y''/H_{yo} = 0$ at ρ_o
k'	k'	τ	$\Delta H_y'/H_{yo}$ at ρe
q_1	y_1	ρ_o	x at ρ_e
ω	ω	ρ_e	$\Delta H_y''/H_{yo} = 0$ at $\rho = 0$
ϕ	ϕ_1		
δ	ρ_δ		

The unknowns that are directly given are B_o k and k' which characterize the "ideal" field. The unknown q_1 may be found from the half gap y_1 using Eq. (2). Tentative choices are made for ω ϕ_1 and ρ_δ. Generally ω must be greater than $\pi/2$ in order to have a maximum x associated with the edge of the pole. If the corresponding y at this location is too large ω must be increased. The value of ϕ_1 must be less than π order that the contour not coincide with the generator surface. For ρ_δ no guide is available but a number around 10 seems to correspond to reasonable yoke locations. Ultimately ϕ_1 and ρ_δ are varied to give the desired pole width and backleg location.

It is to be noted that the central gradient divided by the central field (field index) is

$$\frac{H_y'(0,0)}{H_y(0,0)} = k \, , \tag{18}$$

and that the gradient of the gradient of the field divided by the central field (gradient index) is

$$\frac{H_y''(0,0)}{H_y(0,0)} = k' + \frac{C_1^2}{g_1^2}\,\tau\, G^2(\tau)\left(\frac{d\ln G}{d\xi}\right)_{\xi=\tau} . \tag{19}$$

Furthermore, as may be seen later, Eqs. (18) and (19) are unchanged after the coils are located at finite distances. Hence it is to be noted that the calculated field index and gradient index will equal those calculated from the "ideal" field provided

$$\left(\frac{d\ln G}{d\xi}\right)_{\xi=\tau} = \frac{2-\frac{\omega}{\pi}}{1+\tau} - \frac{\frac{1}{2}}{\delta-\tau} - \frac{1}{\alpha+\tau} - \frac{1}{\gamma+\tau} = 0 . \tag{20}$$

This condition is adopted as a given quantity and appears as the last entry in Table 1. If Eq. (20) is used to solve for γ four unknowns remain: ρ_0 ρ_e α and τ. These may be found from the four remaining given quantities or conditions.

INITIALIZATION OF PARAMETERS

Trial values for ρ_0 ρ_e α τ are calculated from a simplified model[5] in which ξ is considered large with respect to τ but small with respect to 1.

For simplicity the return yoke position is removed to infinity ($\delta = \infty$). Expressions for the first four derivatives of the field at the origin are identical with those of the "ideal" field if

$$\left(\frac{d \ln G}{d\xi}\right)_{\xi=\tau} = \left(\frac{d^2 \ln G}{d\xi^2}\right)_{\xi=\tau} = 0 \ . \tag{21}$$

From Eq. (20) and the assumption that τ is negligible and that $\delta = \infty$, Eq. (21) gives

$$\frac{1}{\alpha_0} + \frac{1}{\gamma_0} = 2 - \frac{\omega}{\pi} \ , \qquad \frac{1}{\alpha_0^2} + \frac{1}{\gamma_0^2} = 2 - \frac{\omega}{\pi} \ . \tag{22}$$

Solving for α_0 and γ_0 one has

$$\frac{1}{\alpha_0} = \frac{1}{2}\left(2 - \frac{\omega}{\pi}\right)\left[1 - \sqrt{1 - 2\,\frac{1-\omega/\pi}{2-\omega/\pi}}\,\right] , \tag{23}$$

and

$$\frac{1}{\gamma_0} = \frac{1}{2}\left(2 - \frac{\omega}{\pi}\right)\left[1 + \sqrt{1 - 2\,\frac{1-\omega/\pi}{2-\omega/\pi}}\,\right] . \tag{24}$$

For the excess over the "ideal" field Eq. (11) gives approximately

$$\frac{\Delta H_y'}{H_{y0}} = \frac{C_1}{g_1}\xi\left(\frac{2-\omega/\pi}{1+\xi} - \frac{1}{\alpha+\xi} - \frac{1}{\gamma+\xi}\right) \equiv \frac{\Delta H'}{H} \ . \tag{25}$$

For convenience let

$$\xi = \eta\,\epsilon \qquad \frac{1}{\alpha} = \frac{1}{\alpha_0} - \epsilon \qquad \frac{1}{\gamma} = \frac{1}{\gamma_0} + \epsilon \ . \tag{26}$$

Then

$$\frac{\Delta H'}{H} = \frac{C_1}{g_1}\,\epsilon^3\eta\left[-2\left(\frac{1}{\alpha_0} - \frac{1}{\gamma_0}\right)\eta + \left(2 - \frac{\omega}{\pi} - \frac{1}{\alpha_0^3} - \frac{1}{\gamma_0^3}\right)\eta^2\right] . \tag{27}$$

At $\eta = \eta$

$$\left(\frac{\Delta H'}{H}\right)_o = \frac{C_1}{g_1}\epsilon^3\eta_o^2\left[-2\left(\frac{1}{\alpha_o}-\frac{1}{\gamma_o}\right)+\left(2-\frac{\omega}{\pi}-\frac{1}{\alpha_o^3}-\frac{1}{\gamma_o^3}\right)\eta_o\right], \tag{28}$$

$$\left[\frac{\partial\left(\frac{\Delta H'}{H}\right)}{\partial\eta}\right]_o = \frac{C_1}{g_1}\epsilon^3\eta_o\left[-4\left(\frac{1}{\alpha_o}-\frac{1}{\gamma_o}\right)+3\left(2-\frac{\omega}{\pi}-\frac{1}{\alpha_o^3}-\frac{1}{\gamma_o^3}\right)\eta_o\right]=0, \tag{29}$$

and at $\eta = \eta_e$

$$\left(\frac{\Delta H'}{H}\right)_e = \frac{C_1}{g_1}\epsilon^3\eta_e^2\left[-2\left(\frac{1}{\alpha_o}-\frac{1}{\gamma_o}\right)+\left(2-\frac{\omega}{\pi}-\frac{1}{\alpha_o^3}-\frac{1}{\gamma_o^3}\right)\eta_e\right]. \tag{30}$$

Since $G(\xi) \cong 1$, Eq. (8) gives

$$C_1 \cong \varphi_1 . \tag{31}$$

From Eq. (29)

$$\eta_o = \frac{4}{3}\cdot\frac{\frac{1}{\alpha_o}-\frac{1}{\gamma_o}}{2-\frac{\omega}{\pi}-\frac{1}{\alpha_o^3}-\frac{1}{\gamma_o^3}} = \frac{8\pi}{3\omega}\cdot\frac{\sqrt{1-2\frac{1-\omega/\pi}{2-\omega/\pi}}}{1-\omega/\pi} . \tag{32}$$

Equation (28) may be solved for ϵ and Eq. (30) then yields η_e by solving a cubic. Equation (26) gives ξ_o and ξ_e. However Eq. (12) by noting that $G(\xi) \cong 1$ gives in particular

$$P_e = \frac{C_1}{g_1}p_e \cong \frac{\varphi_1}{y_1}x_e . \tag{33a}$$

This together with ξ_e may be used in Eq. (13) to give an estimate of τ.

With this value of τ Eq. (13) may again be used to obtain ρ_0

$$\rho_0 \cong \ln\left(\frac{2\xi_0}{\tau}\right). \tag{33}$$

Finally using ε found from Eq. (28), Eq. (26) yields α and γ. In this manner sufficiently accurate trial values for ρ_0 ρ_e α and τ may be found.

ITERATIVE PROCEDURE

If $F(\rho\ \alpha\ \tau)$ designates the gradient in Eq. (11) and $p(\rho\ \alpha\ \tau)$ is given by Eq. (12) then

$$F_0 = F_{000} + \left(\frac{\partial F}{\partial \rho}\right)_{000} \Delta\rho_0 + \left(\frac{\partial F}{\partial \alpha}\right)_{000} \Delta\alpha + \left(\frac{\partial F}{\partial \tau}\right)_{000} \Delta\tau \tag{34}$$

$$\left(\frac{\partial F}{\partial \rho}\right)_0 = \left(\frac{\partial F}{\partial \rho}\right)_{000} + \left(\frac{\partial^2 F}{\partial \rho^2}\right)_{000} \Delta\rho_0 + \left(\frac{\partial^2 F}{\partial \rho \partial \alpha}\right)_{000} \Delta\alpha + \left(\frac{\partial^2 F}{\partial \rho \partial \tau}\right)_{000} \Delta\tau \tag{35}$$

$$F_e = F_{e00} + \left(\frac{\partial F}{\partial \rho}\right)_{e00} \Delta\rho_e + \left(\frac{\partial F}{\partial \alpha}\right)_{e00} \Delta\alpha + \left(\frac{\partial F}{\partial \tau}\right)_{e00} \Delta\tau \tag{36}$$

$$p_e = p_{e00} + \left(\frac{\partial p}{\partial \rho}\right)_{e00} \Delta\rho_e + \left(\frac{\partial p}{\partial \alpha}\right)_{e00} \Delta\alpha + \left(\frac{\partial p}{\partial \tau}\right)_{e00} \Delta\tau , \tag{37}$$

where the values of ρ_0 ρ_e α τ on the right hand side have been assigned trial values. The quantities on the left hand side are specified by the designer. Generally speaking F_0 is the maximum allowed positive excursion from the "ideal" gradient and F_e is the maximum allowed negative excursion from the "ideal" gradient. By definition $\frac{\partial F}{\partial \rho}$ is found using the "ideal" gradient at ρ_0. For example, a zero gradient magnet will have $\frac{\partial F}{\partial \rho} = 0$. The value of p is chosen via Eq. (14) from a value of x equal to the "good field width" for the right or left hand side of the magnet which ever is under consideration. Numerical differentiation is employed to obtain all coefficients. Matrix inversion then gives the increments $\Delta\rho_o$ $\Delta\rho_{\hat{e}}$ $\Delta\alpha$ $\Delta\tau$ which are used to obtain improved trial values. The process is repeated until a suitable convergence criterion is met.

Having found the unknowns for an assumed ϕ_1 and ρ_δ the process is repeated for three additional cases in which ϕ_1 is incremented by a small amount and ρ_δ incremented by a small amount. These four runs are used together with an assumed bilinear variation of x_{max} on the contour and x_{1eg} at the yoke with respect to ϕ_1 and ρ_δ to yield new trial values for ϕ_1 and ρ_δ that will provide given polewidths and yoke positions. This operation is repeated until the changes in x_{max} and x_{1eg} are acceptably small.

After the search mode has been executed and suitable constants found the contour mode is activated by using the parameters found to calculate z on the contour as a function of ρ from Eqs. (16) and (2). On this contour the magnetic field from Eq. (7) and the flux from Eq. (4) are also found. On the median plane Eq. (7) gives the field and Eq. (11) gives the gradient each as a function of ρ which in turn is converted to x using Eqs. (12) and (14).

COMBINED FUNCTION MAGNET WITH COIL

In order to insert a current filament at a finite distance in the w-plane of Figure 4 it is convenient first to transform to the λ-plane using

$$w = \frac{\phi_1}{\pi} \ln \lambda \qquad \text{or} \qquad \lambda = e^{\frac{\pi}{\phi_1} w} . \tag{38}$$

Figure 5 illustrates the current filament at λ_o and its images necessary to preserve the previous constant potential surfaces. The multivalued potential V is represented in the λ-plane as arising from double layers or cuts along the arcs shown. The complex potential for the current filament at λ_o and its images is

$$W = \frac{V_1}{2\pi} \ln \left[\frac{(\lambda_0\lambda - 1)(\lambda_0^*\lambda - 1)}{(\lambda - \lambda_0)(\lambda - \lambda_0^*)} \right] . \tag{39}$$

If $\lambda_0 \to \infty$ Eq. (39) is seen to approach Eq. (4) since from Figure 4 the fraction V_1/V_0 is equal to ϕ_1/π.

For a uniform current density block Eq. (39) may be generalized to

$$W = 2 J_0 \iint \ln \left[\frac{(\lambda_0\lambda - 1)(\lambda_0^*\lambda - 1)}{(\lambda - \lambda_0)(\lambda - \lambda_0^*)} \right] dx_0 dy_0 \tag{40}$$

at least when λ refers to a location outside of the current block which is the present range of interest. The current density is

$$J_0 = \frac{V_1}{4\pi A} , \tag{41}$$

where A is the cross sectional area of the block.

Beth[6] has shown that if h(z) is analytic

$$\iint h(z)\, dx\, dy = \frac{1}{2i} \oint h(z)\, z^* dz , \tag{42}$$

from which it also follows that

$$\iint h(z^*)\, dx\, dy = -\frac{1}{2i} \oint h(z^*)\, z\, dz^* . \tag{43}$$

Now Eq. (40) can be separated into two parts such that Eq. (42) may be applied to the first part and Eq. (43) to the second part. Thus

$$W = \frac{J_0}{i} \oint \ln \left(\frac{\lambda_0\lambda - 1}{\lambda - \lambda_0} \right) z_0^* dz_0 - \frac{J_0}{i} \oint \ln \left(\frac{\lambda_0^*\lambda - 1}{\lambda - \lambda_0^*} \right) z_0\, dz_0^* . \tag{44}$$

A special case of Beth's result gives

$$A = \frac{1}{2i} \oint z_0^* dz_0 = -\frac{1}{2i} \oint z_0\, dz_0^* \tag{45}$$

Hence Eq. (44) becomes

$$W = \frac{V_1}{2\pi} \frac{\oint \ln\left(\frac{\lambda_0\lambda - 1}{\lambda - \lambda_0}\right) z_0^* dz_0}{\oint z_0^* dz_0} + \frac{V_1}{2\pi} \frac{\oint \ln\left(\frac{\lambda_0^*\lambda - 1}{\lambda - \lambda_0^*}\right) z_0 dz_0^*}{\oint z_0 dz_0^*} . \qquad (46)$$

Note that W approaches the expression in Eq. (4) for sufficiently large $|\lambda_0|$
For reference also note that

$$\frac{dW}{d\lambda} = \frac{V_1}{2\pi} \frac{\oint \left(\frac{\lambda_0}{\lambda_0\lambda - 1} - \frac{1}{\lambda - \lambda_0}\right) z_0^* dz_0}{\oint z_0^* dz_0} + \frac{V_1}{2\pi} \frac{\oint \left(\frac{\lambda_0^*}{\lambda_0^*\lambda - 1} - \frac{1}{\lambda - \lambda_0^*}\right) z_0 dz_0^*}{\oint z_0 dz_0^*} , \qquad (47)$$

and

$$\frac{d^2W}{d\lambda^2} = -\frac{V_1}{2\pi} \frac{\oint \left[\left(\frac{\lambda_0}{\lambda_0\lambda - 1}\right)^2 - \left(\frac{1}{\lambda - \lambda_0}\right)^2\right] z_0^* dz_0}{\oint z_0^* dz_0} - \frac{V_1}{2\pi} \frac{\oint \left[\left(\frac{\lambda_0^*}{\lambda_0^*\lambda - 1}\right)^2 - \left(\frac{1}{\lambda - \lambda_0^*}\right)^2\right] z_0 dz_0^*}{\oint z_0 dz_0^*} . \qquad (48)$$

Equation (40) replaces Eq. (4) but the method remains the same except for the additional problem of determining λ_0 from specified locations z_0 on the boundary of the current block.

To begin then, z_0 is given for equally spaced intervals for each segment of the boundary. The corresponding r_0 are found using Eq. (2). Initial guesses for w_0 corresponding to λ_0 are made and r_0 found by integrating Eq. (6) from the origin. These r_0 are compared with the desired r. This change in r_p is translated into a change in w_0 using the differential form of Eq. (6). In this manner improved values for w_0 are made and the process repeated until a convergence criterion is met.

Since Eq. (40) has replaced Eq. (4) the fields now become

$$H^* = i\,\frac{V_0 C_1}{\pi g_1}\,G(s)\left(1 + kz + \tfrac{1}{2}k'z^2\right)C(\lambda)\ , \tag{49}$$

where

$$C(\lambda) = \frac{\lambda}{2}\,\frac{\oint\left(\frac{\lambda_0}{\lambda_0\lambda - 1} - \frac{1}{\lambda - \lambda_0}\right)z_0^* dz_0}{\oint z_0^* dz_0} + \frac{\lambda}{2}\,\frac{\oint\left(\frac{\lambda_0^*}{\lambda_0^*\lambda - 1} - \frac{1}{\lambda - \lambda_0^*}\right)z_0\, dz_0^*}{\oint z_0\, dz_0^*}\ . \tag{50}$$

The complex gradient becomes

$$\frac{dH^*}{dz} = i\,\frac{V_0 C_1}{\pi g_1}\,G(s)\Bigg[(k + k'z)C(\lambda) + \left(1 + kz + \tfrac{1}{2}k'z^2\right)^2 \frac{C_1}{g_1}\,G(s)\cdot \left\{\sqrt{s^2 - \tau^2}\,\frac{d\ln G}{ds}\,C(\lambda) + \frac{\pi}{\phi_1}\left[C(\lambda) - D(\lambda)\right]\right\}\Bigg]\ , \tag{51}$$

where

$$D(\lambda) = \frac{\lambda^2}{2}\,\frac{\oint\left[\left(\frac{\lambda_0}{\lambda_0\lambda - 1}\right)^2 - \left(\frac{1}{\lambda - \lambda_0}\right)^2\right]z_0^* dz_0}{\oint z_0^* dz_0} + \frac{\lambda^2}{2}\,\frac{\oint\left[\left(\frac{\lambda_0^*}{\lambda_0^*\lambda - 1}\right)^2 - \left(\frac{1}{\lambda - \lambda_0^*}\right)^2\right]z_0\, dz_0^*}{\oint z_0\, dz_0^*}\ . \tag{52}$$

On the median plane Eqs. (49) and (51) give

$$\frac{H_y'(x,0)}{H_y(0,0)} = \frac{G(\xi)}{G(\tau)}\,\frac{1}{1 + C(1)}\Bigg[(k + k'x)C(\mu) + \left(1 + kx + \tfrac{1}{2}k'x^2\right)^2 \frac{C_1}{g_1}\,G(\xi)\left\{\sqrt{\xi^2 - \tau^2}\,\frac{d\ln G}{d\xi}\,C(\mu) + \frac{\pi}{\phi_1}\left[C(\mu) - D(\mu)\right]\right\}\Bigg]\ . \tag{53}$$

In general the parameter adjustment for ρ_o ρ_e α and τ proceeds as before except that Eq. (49) replaces Eq. (7) and Eq. (53) replaces Eq. (11). It has been noticed, however, that instabilities occur in taking numerical derivatives of Eq. (53). These instabilities are removed by turning on the change brought about by $C(\mu)$ and $D(\mu)$ very slowly. Thus for the k^{th} iterate and using $C(\mu)$ as an example

$$C_{used}^{(k)} = C_{used}^{(k-1)} + \left[C_{calc}^{(k)} - C_{used}^{(k-1)}\right] \cdot FAC(k), \qquad (54)$$

where

$$FAC(k) = \tanh\left[\frac{.001}{AN(k)}\right]$$

and AN(k) is the root mean square fractional difference in the variables from the $(k-1)^{st}$ iterate. Since the iteration proceeds until AN is less than .0001, the final C_{used} will be very close to C_{calc}.

REFERENCES

1. M.H. Foss, Mathematical Techniques for Designing Field Shapes, Carnegie Inst. Tech., 1951 (NYO-911); see also: W. Hardt, DESY-Bericht A1.5 (1959), R. Perin, CERN Publ. AR/Int SG/64, Geneva, 1964, S. Jaidane, CEA-R-3238 (Rev.), Saclay, 1968.

2. The Preliminary Design of Beijing Proton Synchrotron, Beijing, China, 1979

3. W.R. Smythe, "Static and Dynamic Electricity", 3rd ed., McGraw-Hill Book Co., New York, 1968, p. 82.

4. S.C. Snowdon, IEEE Trans. Nucl. Science, NS-18, 848 (1971).

5. W. Hardt, DESY-Bericht A1.5, Hamburg, 1959, p. 9.

6. R.A. Beth, Journ. Appl. Phys. 38, 4689 (1967); also
R.A. Beth, Journ. Appl. Phys. 40, 2445, 4782 (1969)
K. Halbach, Nucl. Instr. and Meth., 78, 185 (1970)

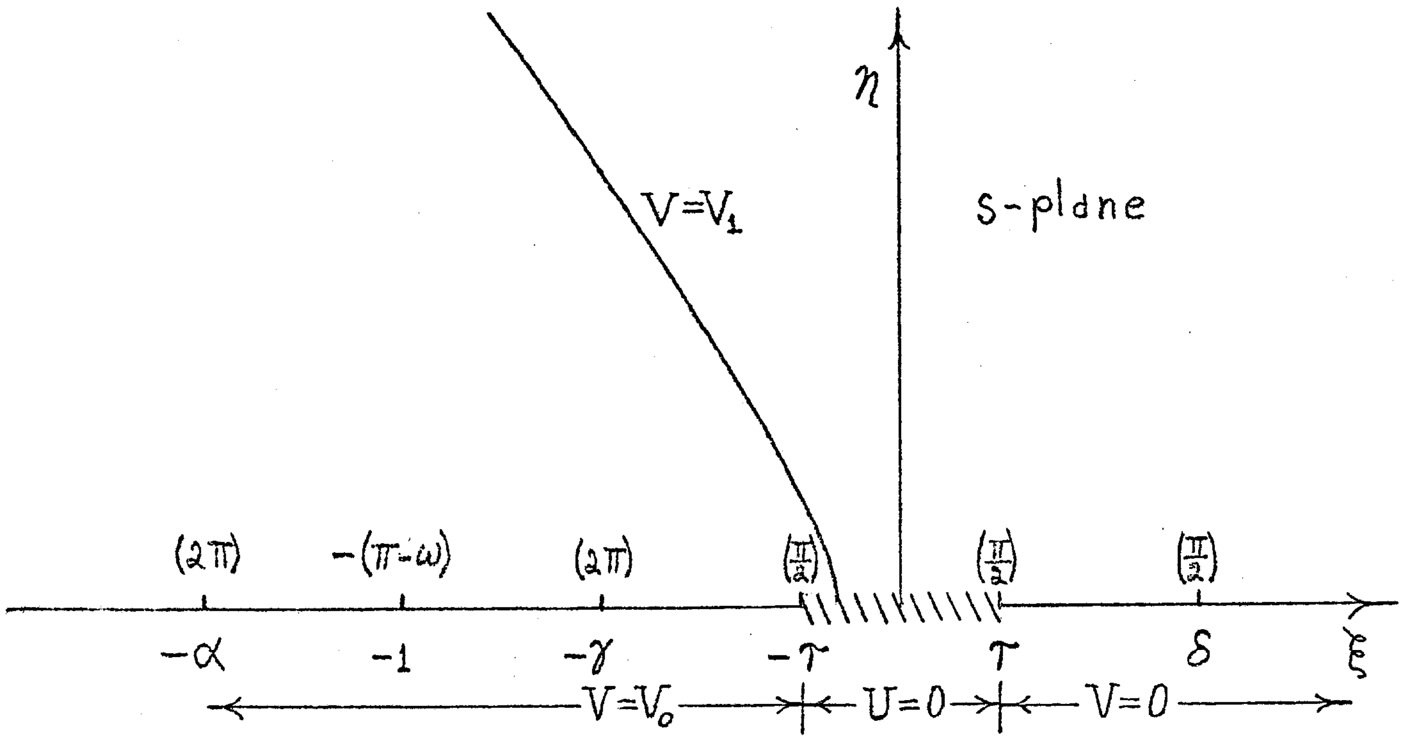

Figure 1. Initial Plane (generators on real axis)

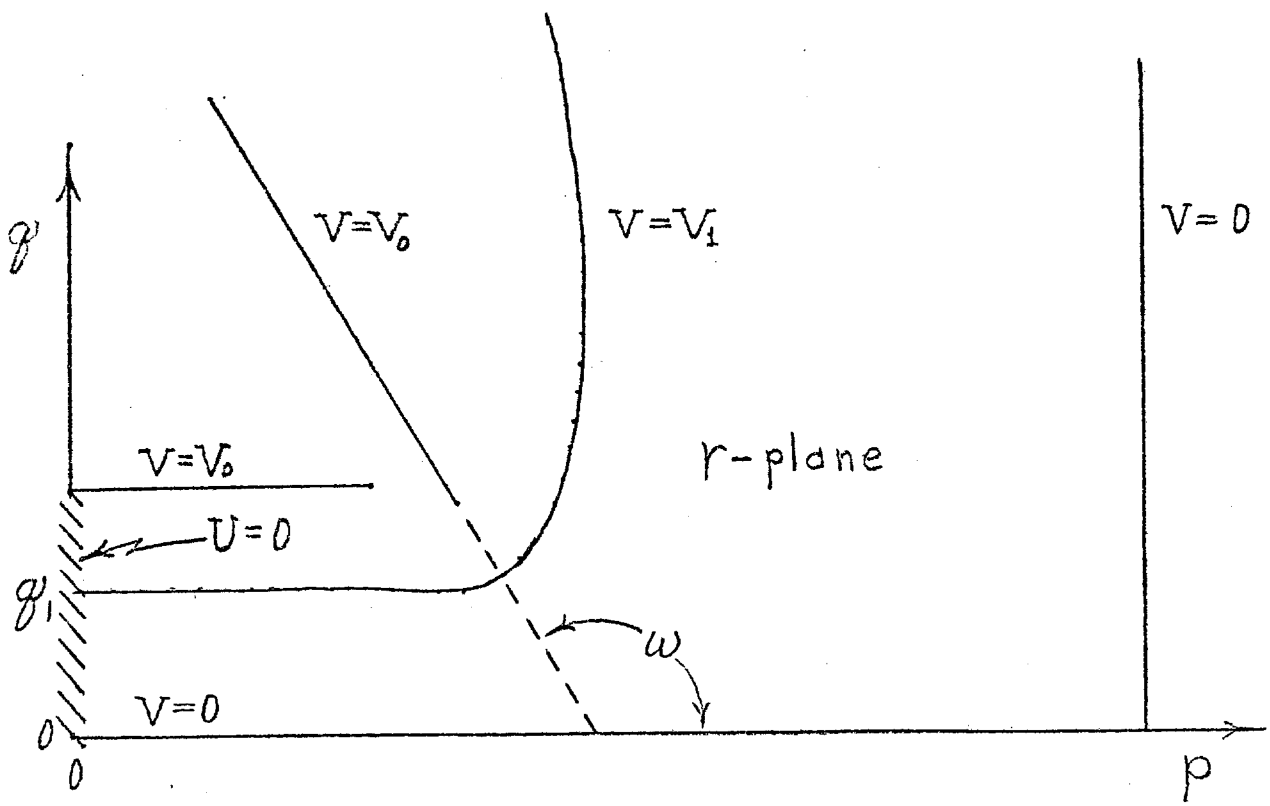

Figure 2. Transformed Plane (straight line generators)

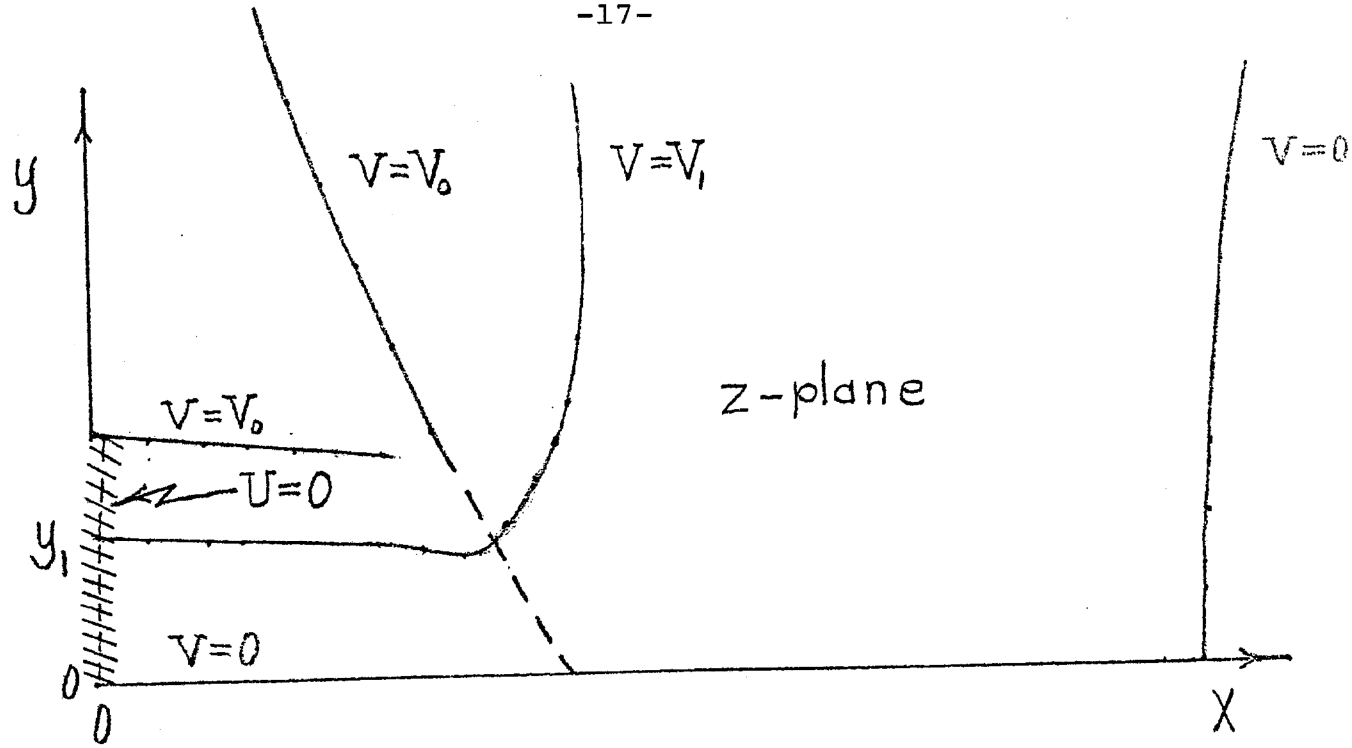

Figure 3. Conformal Mapping (generators distorted)

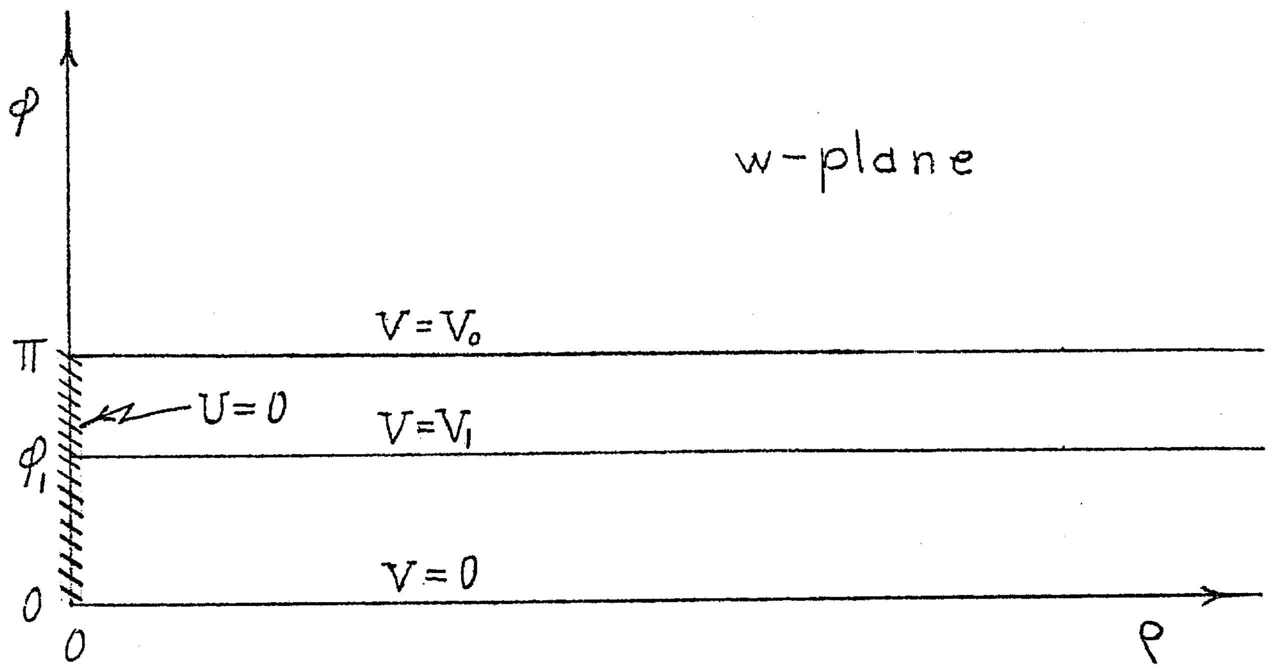

Figure 4. Intermediate Plane (real axis is convenient stepping variable)

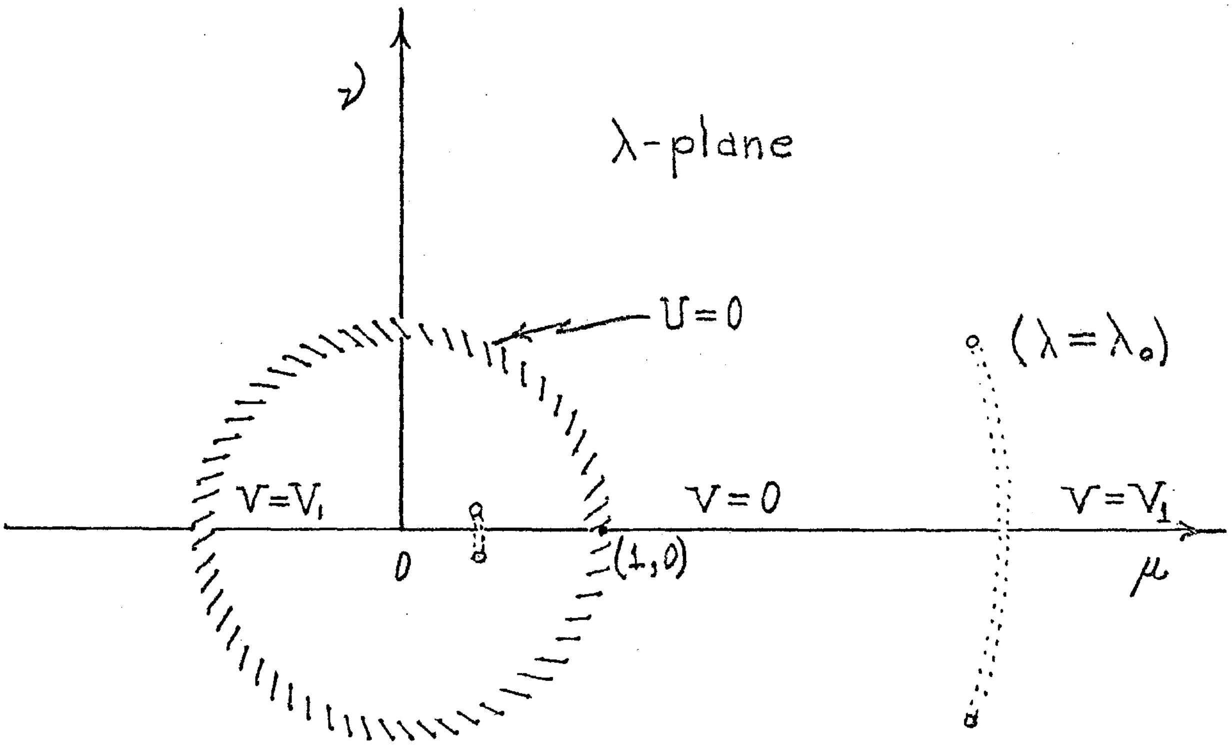

Figure 5. Intermediate Plane (used to specify magnetostatics)